Clinical Cancer Research

Focal Irradiation and Systemic TGFβ Blockade in Metastatic Breast Cancer

Silvia C. Formenti[1], Percy Lee[2,3], Sylvia Adams[4], Judith D. Goldberg[5,6], Xiaochun Li[5,6], Mike W. Xie[2], Josephine A. Ratikan[2], Carol Felix[2], Lin Hwang[3], Kym F. Faull[7], James W. Sayre[8], Sara Hurvitz[3,9], John A. Glaspy[3,9], Begoña Comin-Anduix[3,9], Sandra Demaria[1,10], Dörthe Schaue[2,3], and William H. McBride[2,3]

Abstract

Purpose: This study examined the feasibility, efficacy (abscopal effect), and immune effects of TGFβ blockade during radiotherapy in metastatic breast cancer patients.

Experimental Design: Prospective randomized trial comparing two doses of TGFβ blocking antibody fresolimumab. Metastatic breast cancer patients with at least three distinct metastatic sites whose tumor had progressed after at least one line of therapy were randomized to receive 1 or 10 mg/kg of fresolimumab, every 3 weeks for five cycles, with focal radiotherapy to a metastatic site at week 1 (three doses of 7.5 Gy), that could be repeated to a second lesion at week 7. Research bloods were drawn at baseline, week 2, 5, and 15 to isolate PBMCs, plasma, and serum.

Results: Twenty-three patients were randomized, median age 57 (range 35–77). Seven grade 3/4 adverse events occurred in 5 of 11 patients in the 1 mg/kg arm and in 2 of 12 patients in the 10 mg/kg arm, respectively. Response was limited to three stable disease. At a median follow up of 12 months, 20 of 23 patients are deceased. Patients receiving the 10 mg/kg had a significantly higher median overall survival than those receiving 1 mg/kg fresolimumab dose [hazard ratio: 2.73 with 95% confidence interval (CI), 1.02–7.30; $P = 0.039$]. The higher dose correlated with improved peripheral blood mononuclear cell counts and a striking boost in the CD8 central memory pool.

Conclusions: TGFβ blockade during radiotherapy was feasible and well tolerated. Patients receiving the higher fresolimumab dose had a favorable systemic immune response and experienced longer median overall survival than the lower dose group. *Clin Cancer Res; 24(11); 2493–504. ©2018 AACR.*

Introduction

TGFβ is a pleiotropic cytokine that maintains homeostasis in many organ systems by limiting the growth of epithelial, endothelial, neuronal, and hematopoietic cell lineages (1–4). TGFβ is secreted by cells in a biologically inactive form by virtue of its association with latency-associated protein (LAP) and stored in the extracellular matrix as a complex.

TGFβ suppresses the growth of epithelial cells, including those in the early stages of tumor development (premalignant conditions), but in advanced cancers TGFβ promotes tumor growth and metastasis, through increased tumor cell motility, migration, and invasiveness (1, 4). Increased production of TGFβ was demonstrated in many neoplasms including breast cancer, and elevated plasma TGFβ levels in patients correlate with worse outcome (5–7).

In addition, TGFβ alters the tumor microenvironment and has broad immune suppressive activity across natural killer (NK) cells, T cells, and myeloid cells. TGFβ hinders the initiation of immune responses and the development of antitumor effector cells (8–12). Neutralizing antibodies can reverse TGFβ-mediated immune suppression, favoring activation of NK- and T cell-mediated tumor rejection (8–10, 12, 13). Thus, blocking TGFβ merges the advantages of disrupting a key promoter of tumor growth with those of counteracting immune-suppression.

Our group introduced the notion of combining radiotherapy (RT) and immunotherapy in the treatment of cancer (14), the underlying idea for this trial. Radiation generates "danger" signals in tissues (15), that, under certain conditions, enhance immune presentation of tumor antigens liberated from radiation-damaged cells, thus working as a vaccine (16). Ionizing radiation induces TGFβ activation *in vitro* and *in vivo*, in normal and cancer cells (17–21), at least in part through a redox mechanism that acts directly on the secreted latent protein (22). The recognition that radiation triggers activation of TGFβ, which in turn promotes DNA damage repair, mediates EMT and suppresses antitumor

[1]Department of Radiation Oncology, Weill Cornell Medical College, New York, NY. [2]Department of Radiation Oncology, University of California, Los Angeles, California. [3]Jonsson Compressive Cancer Center, University of California, Los Angeles, California. [4]Department of Medicine, New York University School of Medicine, New York, NY. [5]Department of Population Health, New York University School of Medicine, New York, NY. [6]Department of Environmental Medicine, New York University School of Medicine, New York, NY. [7]Pasarow Mass Spectrometry Laboratory at University of California, Los Angeles, California. [8]Public Health Biostatistics at University of California, Los Angeles, California. [9]Medicine, Hematology & Oncology at University of California, Los Angeles, California. [10]Department of Pathology and Laboratory Medicine, Weill Cornell Medical College, New York, NY.

Note: Supplementary data for this article are available at Clinical Cancer Research Online (http://clincancerres.aacrjournals.org/).

D. Schaue and W.H. McBride have equal contributions.

Corresponding Authors: William H. McBride, UCLA, Room B3-109, Los Angeles, CA 90095-1714. Phone: 310-794-7051; Fax: 310-206-1260; E-mail: wmcbride@mednet.ucla.edu; and Silvia C. Formenti, Department of Radiation Oncology, 525 East 68th Street, Box 169, New York NY 10065. Phone: 212-746-3600; Fax: 212-746-8749; E-mail: formenti@med.cornell.edu

doi: 10.1158/1078-0432.CCR-17-3322

Translational Relevance

Many human tumors present with an active TGFβ signature that drives a therapy-resistant phenotype with an increased propensity for epithelial–mesenchymal transition, and for immune escape. This study asked whether TGFβ blockade in combination with local radiation in patients with metastatic breast cancer could improve survival and the immune landscape. A multicentric prospective pilot trial randomized chemo-refractory metastatic breast cancer patients to two doses of fresolimumab (1 or a 10 mg/kg), and focal radiation to one metastatic site. Favorable changes in circulating PBMC levels, and in memory CD8 T cells coincided with median overall survival benefits of the patients treated at the higher dose. Combining radiation with sufficient TGFβ blockade can create a systemic immune landscape that might allow T cells to escape the suppressive grip of TGFβ.

effector cells provides a strong rationale for testing TGFβ inhibition during radiotherapy (23).

Fresolimumab (GC1008) is a human IgG4 kappa monoclonal antibody that neutralizes all mammalian isoforms of TGFβ (i.e., β1, β2, and β3) with half-life ranging from 21 to 30 days (24). Supported by our preclinical data in mouse models of metastatic breast cancer (25, 26), we conducted a clinical trial to test in metastatic breast cancer patients, with tumors refractory to standard treatment, the feasibility and efficacy of combining TGFβ blockade by fresolimumab with focal radiotherapy, while performing immunomonitoring in peripheral blood.

Materials and Methods

Study design

This study (NCT01401062) was conducted in accordance with recognized ethical guidelines as embodied in the Declaration of Helsinki and was approved by the Institutional Review Boards of both UCLA and NYU. Informed consent was obtained from each subject prior to entry into the trial.

The study was an open label randomized trial at two centers (Supplementary Fig. S1). Fresolimumab was administered under IND I111874. Patients with metastatic breast cancer after at least one course of systemic therapy who had evidence of disease progression at two consecutive clinical/radiological assessments (at an interval of at least 2 weeks) and at least three distinct metastatic sites were eligible for enrollment. After informed consent, patients were randomized within site by the biostatistics shared resource (BSR) of NYU Cancer Institute using established procedures to either 1 or 10 mg/kg of fresolimumab. Imaging by PET/CT was performed at baseline, 5 and 15 weeks. The study drug was administered every 3 weeks (weeks 0, 3, 6, 9, 12). A metastatic site was chosen to receive conformal external beam radiation of 3 fractions of 7.5 Gy, to a total of 22.5 Gy, on alternating days over the course of week 1 and 7. In patients in which two lesions were available, lesion 1 was irradiated at week 1 (RT started 1 week after first dose of fresolimumab); lesion 2 was irradiated at week 7, starting 1 week after the third dose of fresolimumab. Fresolimumab was administered as intravenous infusions, after premedication with diphenhydramine and acetaminophen. Response was assessed at week 15 and patients were followed until death. The primary endpoint of the study was abscopal response at week 15 based on Immunological Response Criteria (irC; ref. 27). The sum of the longest diameter (LD) for all target lesions was calculated and reported as the baseline sum LD.

Chemicals

Ficoll-Paque (GE Healthcare Bio-Sciences), human AB serum (OmegaSci), FBS (Sigma-Aldrich), dimethyl sulfoxide and DNAse (Sigma), RPMI1640 medium with L-glutamine (Mediatech, Inc.) were used.

Sample collection

Approximately 60 mL of blood was drawn into heparinized BD vacutainer tubes (BD Bioscience) at baseline, after the first cycle of antibody infusion and radiation (week 2), after the second cycle of antibody infusion (week 5) and after completion of treatment (week 15) and processed for isolation of peripheral blood mononuclear cells (PBMC) by gradient centrifugation within 3 hours of blood draw and controlled-rate frozen in aliquots in human AB serum containing 10% (v/v) DMSO at −80°C before storage in liquid nitrogen. Additionally, a SST serum tube and a CTAD plasma tube were also drawn and processed according to manufacturer's recommendation before storage in aliquots at −80°C. Batches of frozen PBMCs, serum, and plasma were shipped between UCLA and NYU overnight on dry ice. PBMCs from 11 healthy volunteers were isolated on Ficoll-Paque Premium at UCLA as above and served as controls.

Multimer-binding assay and immunophenotyping

Serial samples of individual patients were assayed on the same day for dextramer binding and for levels of 20 major immunophenotype markers (28). PBMCs were thawed by dilution in prewarmed RPMI1640 medium with 10% (v/v) FBS, treated with DNAse, washed and resuspended in PBS.

HLA-A*0201 positivity was confirmed by staining 1 to 2×10^5 PBMCs in 2% FBS/PBS staining buffer (BD Pharmingen) with 1 μL of BB515 anti-HLA-A2 antibody for 30 minutes at 4°C and analyses by flow cytometry (LSRFortessa; BD Biosciences). A total of 1×10^6 aliquots from HLA-A*0201-positive subjects were tested for binding of HLA-A2-restricted survivin-specific dextramers and prepared with fixable viability stain 510 (BD Horizon) according to manufacturer's instructions prior to incubation with 10 μL of the MHC dextramer-PE for the HLA-A2-restricted survivin epitope Sur1M2 (LMLGEFLKL; Immudex) in 5% FBS/PBS (29, 30). Alternatively, a tetramer with the identical survivin epitope (Beckman Coulter) was used. Sample volume permitting, an additional 1×10^6 aliquot was stained with a MHC dextramer mix containing 10 μL of each of the HLA-A2-restricted epitopes for Jarid1B (QLYALPCVL-FITC), Mucin-1 (STAPPVHNV-PE), and Her2/neu (KIFGSLAFL-APC; Immudex; refs. 31–36). After an initial 10 minutes room temperature incubation with the dextramers, 4 μL PerCP-Cy5.5 anti-CD8 (clone RPA-T8) was added for an additional 20 minute incubation on ice before washing and flow cytometric analysis. A total of 2 to 3×10^5 events were collected and analyzed with FlowJo (Supplementary Methods S1; Supplementary Table S1). Quality control required ≥10,000 viable events and ≥2,000 $CD8^+$ T cells. PBMCs from a single healthy volunteer with confirmed HLA-A*0201^+ status served as staining control at all times (internal control). The arbitrary nature of the dextramer/tetramer $CD8^+$ gating was addressed by setting a consistent 0.03% lower limit according to the historic binding of the negative tetramer to the internal control (30, 37). The resulting average positivity of this control sample reached 0.122% ± 0.082

survivin reactive $CD8^+$ T cells, which was also adopted for dextramer staining.

PBMCs from all subjects, regardless of the HLA status, were assayed for surface markers in 2 separate 11 and 12 color panels to capture major T cells subsets (panel 1) as well as B cells, monocytes, myeloid-derived suppressor cells (MDSC), dendritic cells (DC) and NK cells (panel 2; Supplementary Methods S1; Supplementary Table S1; ref. 28). A total of 2 to 4×10^6 aliquots of PBMCs from all subjects were prepared with fixable viability stain 510, as above, prior to assaying for surface markers. Panel 1 was premixed in brilliant stain buffer (BD Horizon/BD Biosciences) containing FITC anti-human CD4, PE anti-human CD25, PE-CF594 anti-human CXCR3, PerCP-Cy5.5 anti-human CD3, PE-Cy7 anti-human CD127, APC anti-human CD45RA, Alexa Flour 700 anti-human CD8, BV421 anti-human PD-1, and BV650 anti-human CCR6 (Supplementary Table S1). A total of 1 to 2×10^6 cells in 50 μL 2% FBS/PBS staining buffer were heat activated at 37°C in the presence of BV605 anti-human CCR7 alone before 20 minutes at room temperature with all other antibodies. Washed cells were analyzed within 2 hours and 1 to 2×10^5 events collected on a LSRFortessa with UltraComp eBeads compensation (eBioscience, Inc.). The second panel comprised FITC anti-human HLA-DR, PE anti-human CD14, PE-CF594 anti-human CD56, PerCP-Cy5.5 anti-human CD11b, PE-Cy7 anti-human CD19, APC anti-human CD15, Alexa Flour 700 anti-human CD11c, APC-H7 anti-human CD20, BV421 anti-human CD123, BV510 anti-human CD3, and BV650 anti-human CD16 (Supplementary Table S1) premixed in brilliant stain buffer as above. A total of 1 to 2×10^6 cells were stained in 50 μL 2% FBS/PBS staining buffer for 30 minutes at room temperature, washed and submitted to flow cytomety as above. FlowJo was used for a gating strategy based on Maecker and colleagues (Supplementary Figs. S2 and S3; ref. 28). Quality control required ≥50% viability and ≥2,000 $CD3^+CD8^+$, $CD3^+CD4^+$ T cells and/or ≥2,000 viable myeloid cells and PBMCs from one volunteer served as an internal control (see above).

Plasma levels of tryptophan and kynurenine

Frozen CTAD-treated plasma was tested for tryptophan and kynurenine by liquid chromatography/tandem mass spectrometry based on a method by Midttun and colleagues (38). Solutions of internal standards, namely 500 pmol $^2H_5$-kynurenine and 2 nmol $^2H_3$-tryptophan, both in 10 μL of water, were added to 100 μL aliquots of plasma and vigorously mixed. Samples were then treated with 300 μL methanol, vigorously mixed again followed by a 30-minute incubation at RT. After a 5-minute centrifugation at 16,060 × *g*, the supernatants were transferred to clean microcentrifuge tubes and dried in a vacuum centrifuge. Dilute hydrochloric acid (0.1N, 100 μL) was added to the dried residues and then vigorously agitated. These samples were centrifuged again for 5 minutes at 16,060 × *g* (RT) and supernatants transferred to LC injector vials. Five microliters of aliquots of the supernatants were injected onto a reverse-phase HPLC column (Scherzo C18 100 × 2.1 mm, 1.7 μm particle size and 100 Å), equilibrated in solvent A (water/acetonitrile/formic acid, 100/3/0.1, all by vol) and eluted (200 μL/min) with an increasing concentration of solvent B (45 mmol/L ammonium formate/acetonitrile, 65/35, vol/vol: min/%B; 0/0, 5/0, 30/32, 35/0, 45/0). The effluent from the column was directed to an electrospray ion source connected to a triple quadrupole mass spectrometer (Agilent 6460) operating in the positive ion multiple reaction monitoring (MRM) mode. The intensities of peaks in selected MRM transitions were recorded at previously determined retention times and optimized instrumental settings [kynurenine m/z 209.0⇒192.0 at retention time (rt) 20.6 minutes; $^2H_5$-kynurenine m/z 214.0⇒96.0 at rt 20.6 minutes; tryptophan m/z 205.0⇒188.0 at rt 22.4 minutes; $^2H_3$-tryptophan 208.0⇒147.0 at rt 22.4 minutes].

The samples were divided into four batches (23 samples/batch), each sample was analyzed in duplicate, and each batch included 10 standards (five dilutions, each in duplicate). The standards were prepared as above with pH 7.2 PBS substituting for plasma, the same amount of internal standards, and increasing amounts of kynurenine (0, 50, 100, 200, and 400 pmol) and tryptophan (0, 1.25, 2.5, 5, and 10 nmol). The data from the standards were used to construct standard curves in which the ratio of peak intensities (ordinate; kynurenine/$^2H_5$-kynurenine or tryptophan/$^2H_3$-tryptophan) was plotted against amount of kynurenine or tryptophan (abscissa); the kynurenine and tryptophan content of each sample was interpolated from the respective standard curves. The values for the duplicate samples were averaged. The limit of detection for kynurenine and tryptophan was around 50 fmol injected.

Humoral immune responses

Frozen serum samples drawn at baseline, week 5 and week 15 were shipped on dry ice to Serametrix Corp. and tested for antibody reactivity against 34 different putative tumor-antigens, namely CABYR, CSAG2, CTAG1B, CTAG2, CYCLINB1, CYCLIND1, GAGE1, HER2, HSPA4, HSPD1, HTERT, LDHC, MAGEA1, MAGEA3, MAGEB6, MICA, MUC1, MYCPB, NLRP4, P53, PBK, PRAME, SILV, SPANXA1, SSX2, SSX4, SSX5, SURVIVIN, TRIP4, TSSK6, TULP2, WT-1, XAGE and ZNF165. A positive score was returned for any measurement that was above 2× the 25th percentile of all antigens, patients and time points.

Statistical methods

Twenty-eight patients with metastatic breast cancer were to be randomized within each of the two study sites (NYU and UCLA) to arm 1 or arm 2 and were to be followed for evaluation of abscopal responses based on irC at 15 weeks. Each arm is considered separately in this report. With 14 patients in a single arm, we could test the null hypothesis that the abscopal response rate is less than or equal to 2% versus the alternative that the response rate is 20% or greater with a power of 80% and two-sided $\alpha = 0.032$ (target = 0.05) using a single stage design (calculations from PASS, NCSS, 2008). If we observed 2 or more abscopal responses in these 14 patients, we could conclude that the dose/schedule of the arm is feasible.

The baseline characteristics of patients were summarized using descriptive statistics. Fisher exact tests were used to compare the distributions of the qualitative variables between the two arms, and two sample t tests were used to compare the means of the quantitative variables between the two arms. No adjustments for multiple testing were used. The overall survival of patients in the two arms was compared with a log-rank chi-square test and the hazard ratio of the two groups was provided with 95% CI.

A repeated measures analysis of variance was used to assess differences between patients for each serological marker at baseline and for each patient over time of treatment, expressed as $\log_2$ fold changes ($\log_2$[value/value at baseline]). Longitudinal

immune responses for each patient were assessed in the context of survival data and summarized through quantile regression and compared as cohorts of the two treatment arms with the Wilcoxon test. Statistical significance was at the 5% level.

Results

Study patients

Among 53 patients who were screened 24 were eligible and 23 were randomized in the study: 16 at NYU and 7 at UCLA. One patient withdrew consent before entering the study. Reason for exclusion of 29 patients included ascites, unstable brain metastases, ongoing anticoagulant therapy, poor liver function, and only one site of measurable disease. The trial stopped after 23 patients were accrued because fresolimumab was no longer available. Among the 23 patients who were treated 11 were randomized to 1 mg/kg of fresolimumab (arm 1; eight at NYU; three at UCLA) and 12 to 10 mg/kg (arm 2; eight at NYU, four at UCLA; Fig. 1). There were no significant differences in the distributions of the baseline patient characteristics, between the two arms (Table 1). All patients' tumors had demonstrated progression to at least two previous treatment lines (range 2–7).

Toxicity of combined radiotherapy and fresolimumab

For both arms toxicity was acceptable. Overall, seven Grade 3–4 adverse events possibly related to treatment occurred in 5 of 11 patients in arm 1 and in 2 of 12 patients in arm 2, respectively. The only grade 4 toxicity was fatigue, observed in one patient in each arm. Grade 3 toxicities occurred in 4 of 11 patients assigned to arm 1 but and consisted of liver enzyme elevations in three patients and anemia in one patient. Fatigue was the only grade 3 toxicity among the 12 patients in arm 2 (Supplementary Table S2). Grade 1 skin lesions, in the form of keratoacanthoma or "keratoacanthoma-like" squamous cell carcinomas (Fig. 2) were observed in 2 of 23 patients and occurred only among patients assigned to the higher dose of fresolimumab.

Response to combined radiotherapy and fresolimumab

Objective responses were limited to stable disease in one patient in arm 1 and 2 patients in arm 2. Figure 2 describes one patient with stable disease who had triple negative breast cancer that had progressed after five lines of chemotherapy. The first radiation course during fresolimumab treated a liver metastasis, and the second course a breast metastasis. At week 15, the patient achieved a 28% reduction of un-irradiated lesions without any new lesions, consistent with a limited abscopal response during irSD. She maintained stable disease for 12 months, until she succumbed to AML, likely anthracycline-induced based on cytogenetics assessment.

Despite the general lack of abscopal responses, patients in arm 2 had significantly lower risk of death compared with arm 1 (HR arm 1 to arm 2: 2.73 with 95% CI, 1.02–7.30; $P = 0.039$; Fig. 2F). There were 11 deaths in arm 1 and the median survival time in this group was 7.57 months (95% CI, 1.67–14.93 months); and there were nine death events in arm 2 and the median survival time was 16.0 months (95% CI, 1.57–55.03 months).

Basic blood composition

Most patients had PBMC's counts that were well below the healthy cohort (Supplementary Fig. S4A), median (med), and interquartile range (IQR) 0.9 ± 0.48 versus 1.9 ± 0.45; $P = 0.001$, although still within normal range ($0.8–3.2 \times 10^6$/mL). Interestingly, seven of nine patients in the 10 mg/kg-arm responded with stable or rising PBMC counts whereas only 5 of 10 did when treated with 1 mg/kg ($W = 70.0/P = 0.051$; Fig. 3A).

Tumor-specific $CD8^+$ T cells

Survivin was chosen as a surrogate universal tumor-specific antigen. Of 22 patients available for immune monitoring, 11

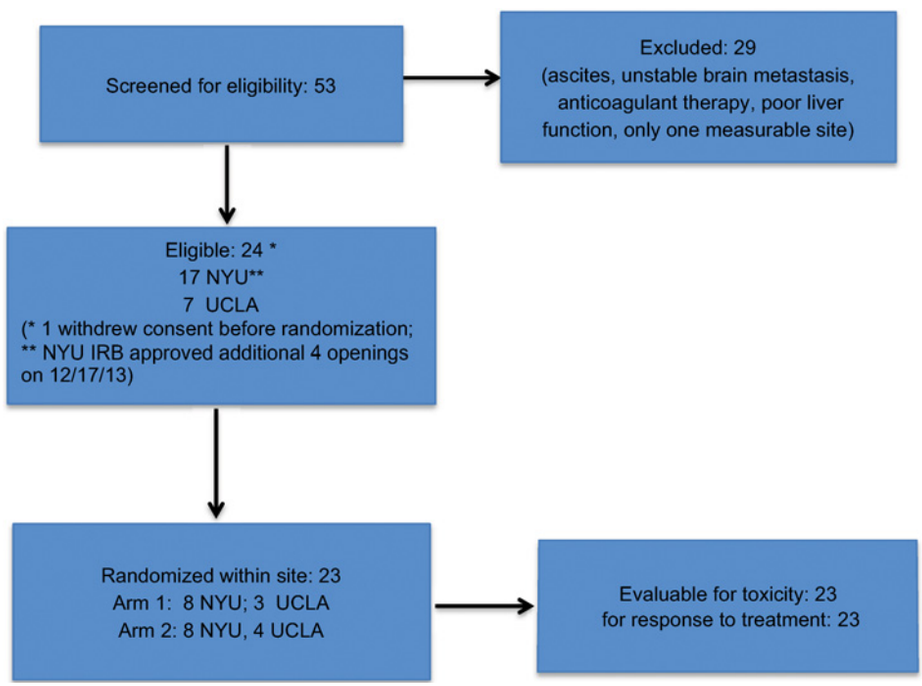

Figure 1.
Consort flow diagram.

Table 1. Patient characteristics by treatment arm and site (NYU: $n = 16$; UCLA: $n = 7$)

		Arm 1 (1 mg/kg, $n = 11$)		Arm 2 (10 mg/kg, $n = 12$)			Total ($n = 23$)	
Variable	**Site**	**Mean (SD)**	**Median (range)**	**Mean (SD)**	**Median (range)**	***P* value *T* test**	**Mean (SD)**	**Median (Range)**
Age	NYU	49.3 (12.4)	49 (35–72)	62.4 (12.1)	64 (43–75)	0.051	55.8 (13.7)	56 (35–75)
	UCLA	65.7 (10.0)	62 (58–77)	54.8 (8.5)	52 (49–67)	0.203	59.4 (10.2)	58 (49–77)
	Total	53.7 (13.7)	55 (35–77)	59.8 (11.3)	59 (43–75)	0.259	56.9 (12.6)	57 (35–77)
Fresolimumab infusions	NYU	3 (1.3)	3 (1–5)	3.4 (1.8)	4 (1–5)	0.638	3.2 (1.5)	3.5 (1–5)
	UCLA	2.7 (2.1)	2 (1–5)	4.8 (0.5)	5 (4–5)	0.222	3.9 (1.7)	5 (1–5)
	Total	2.9 (1.5)	3 (1–5)	3.8 (1.6)	4.5 (1–5)	0.159	3.4 (1.6)	4 (1–5)
Ethnicity			No (%)		No. (%)	Fisher exact test		No. (%)
	NYU	Asian	0 (0)	Asian	0 (0)	0.467	Asian	0 (0)
		Black	2 (25)	Black	0 (0)		Black	2 (12.5)
		Other	0 (0)	Other	1 (12.5)		Other	1 (6.3)
		White	6 (75)	White	7 (87.5)		White	13 (81.3)
	UCLA	Asian	1 (33.3)	Asian	2 (50)	1.0	Asian	3 (42.9)
		Black	1 (33.3)	Black	0 (0)		Black	1 (14.3)
		Other	0 (0)	Other	0 (0)		Other	0 (0)
		White	1 (33.3)	White	2 (50)		White	3 (42.9)
	Total	Asian	1 (9.1)	Asian	2 (16.7)	0.328	Asian	3 (13)
		Black	3 (27.3)	Black	0 (0)		Black	3 (13)
		Other	0 (0)	Other	1 (8.3)		Other	1 (4.4)
		White	7 (63.6)	White	9 (75)		White	16 (69.6)
Tumor type	NYU[a]	Ductal	5 (71.4)	Ductal	5 (71.4)	1.0	Ductal	10 (71.4)
		Lobular	2 (28.6)	Lobular	2 (28.6)		Lobular	4 (28.6)
	UCLA	Ductal	3 (100)	Ductal	4 (100)	1.0	Ductal	7 (100)
		Lobular	0 (0)	Lobular	0 (0)		Lobular	0 (0)
	Total	Ductal	8 (80)	Ductal	9 (81.8)	1.0	Ductal	17 (81)
		Lobular	2 (20)	Lobular	2 (18.2)		Lobular	4 (19.1)
Tumor molecular subtype[b]	NYU	HR+	4 (50)	HR+	6 (75)	0.765	HR+	10 (62.5)
		HR+HER2+	1 (12.5)	HR+HER2+	0 (0)		HR+HER2+	1 (6.3)
		HR-HER2+	1 (12.5)	HR-HER2+	0 (0)		HR-HER2+	1 (6.3)
		TN	2 (25)	TN	2 (25)		TN	4 (25)
	UCLA	HR+	1 (33.3)	HR+	1 (25)	0.657	HR+	2 (28.6)
		HR+HER2+	1 (33.3)	HR+HER2+	0 (0)		HR+HER+	1 (14.3)
		HR-HER2+	0 (0)	HR-HER2+	0 (0)		HER2+	0 (0)
		TN	1 (33.3)	TN	3 (75)		TN	4 (57.1)
	Total	HR+	5 (45.5)	HR+	7 (58.3)	0.367	HR+	12 (52.2)
		HR+HER2+	1 (18.2)	HR+HER2+	0 (0)		HR+HER2+	2 (8.7)
		HR-HER2+	1 (9.1)	HR-HER2+	0 (0)		HR-HER2+	1 (4.4)
		TN	3 (27.3)	TN	5 (41.7)		TN	8 (34.8)

[a]Tumor type was not available for one patient in each arm.
[b]HR, hormone receptor; TN, triple negative.

(50%) were HLA-A*0201 positive and therefore eligible for the multimer binding assay as were 6 of 11 healthy controls (54.5%). One patient (N01) had a significant treatment delay of almost 9 months before starting again with the full course (N01*), which led to repeated blood draws at baseline and week 2. In total, there were 12 samples at baseline, 10 samples each at week 2 and 5, and 5 samples remaining by week 15. The threshold for positivity was based on healthy controls having a med/IQR of survivin-reactive $CD8^+$ T cells of 0.12+0.06% (Fig. 3B). At baseline, excluding one who did not go past week 2, there were 3 of 11 patients (27%), namely N01, N03, and N05, all in the 1 mg/kg GC1008 arm, who had preexisting levels of survivin-reactive $CD8^+$ T cells above the threshold which increased further during treatment in a couple of cases. The third patient, N05, experienced a transient decline in survivin-specific $CD8^+$ T cells during the trial before returning to near pretreatment levels by week 15. The majority of patients maintained survivin-specific $CD8^+$ T cell levels within the normal, negative range throughout the course of treatment with the exception of patients N02, N03, N014, and U03 who had positive values at least at one point, either during or at the end of treatment (Fig. 3B), although such responses were weak compared to those with preexisting levels.

A small number of patients (6) were tested for reactivity towards other, putative tumor antigens Muc-1, Her2/neu, and Jarid1B (Supplementary Table S3; refs, 31–36). Remarkably, four to five patients (80%) had preexisting T-cell reactivity against JARID1B considering the healthy volunteer's values as the lower limit (0.11+0.02%, see above). The frequency of these cells appeared to fluctuate significantly during treatment but remained above the threshold for the most part (Supplementary Fig. S4B). Only two patients (40%) had anti-Her2 T-cell reactivity at baseline (N10 and U07, cut-off = 0.17%), and both fell progressively during treatment. Meaningful Muc1-specific T-cell levels (cut-off =0.17%) could be detected in two individuals before treatment (N10 and N14) but only one patient (N14) was able to respond with a transient Muc-1 T-cell spike at week 2. In fact, patient N14 appeared to respond with a transient rise in tumor-specific T cells for all four tumor antigens (Supplementary Table S3). Clearly, the number of patients in each treatment arm is insufficient to evaluate any epitope spreading.

Humoral responses

Antibody-responses against 34 putative tumor-antigens were limited in this set of patients and they mostly failed to change

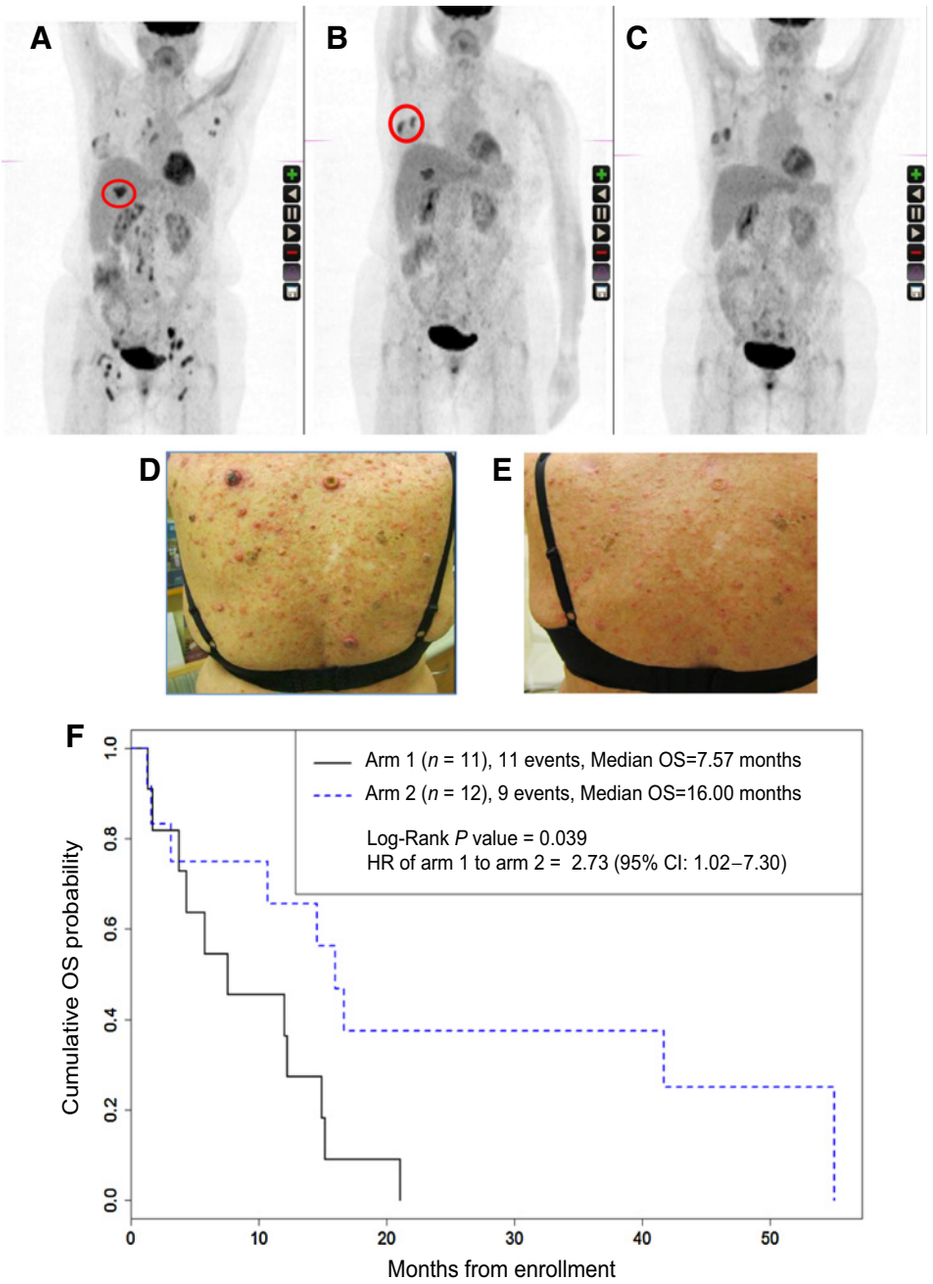

Figure 2.
Response to treatment. **A–E**, Example of response and skin toxicity. A 69 y.o. caucasian woman with TNBC, who had progressed after five lines of systemic chemotherapy was randomized to arm 2. **A,** PET/CT before treatment, showing the lesion in the liver that was chosen for irradiation on week 1 (red circle). **B,** PET/CT on week 5, and breast metastasis that was chosen for irradiation (red circle) on week 7. **C,** Abscopal response in left axilla and bilateral iliac and inguinal nodes, without new lesions, irSD (28%), last PET/CT on week 15. **D,** Development of skin keratoacanthomas during treatment. **E,** Resolution of skin keratoacanthoma at week 15. **F,** Overall survival by arm of the study.

significantly following treatment (Supplementary Table S4). Four patients had preexisting responses to >5 of these antigens. Two of these patients, namely N09 and N03 significantly decreased their tumor-specific antibody load with time and both were in the 1 mg/kg arm. Of the remaining 11 patients who started with low antibody reactivity, three increased in responsiveness to a score of >1 and all three had received 10 mg/kg doses (U03, N11, and U05). Of note, the two patients who converted to positive survivin-specific responses in the tetramer analysis (U03 and N02, Fig. 3B) also had rising survivin antibody titers (not shown). Patient N03 had both high preexisting survivin-specific T cells (Fig. 3B) and preexisting survivin-reactive antibodies (not shown) but T- and B-cell responses against survivin were generally not correlated (not shown).

Memory subsets

Analysis of 10 patients for CD45RA and CCR7 expression revealed the classic T-cell differentiation along the naïve–effector–memory axis, with many effector cells in the CD8 compartment (Fig. 3C) but relatively few in the CD4 T-cell pool (Fig. 3D). Perhaps the most striking finding in the 10 mg/kg fresolimumab treatment group was an increase in the memory pool, especially of the central memory type. This came largely at the expense of effector CD8 cells and stood in stark contrast to the responses in the 1 mg/kg arm where the

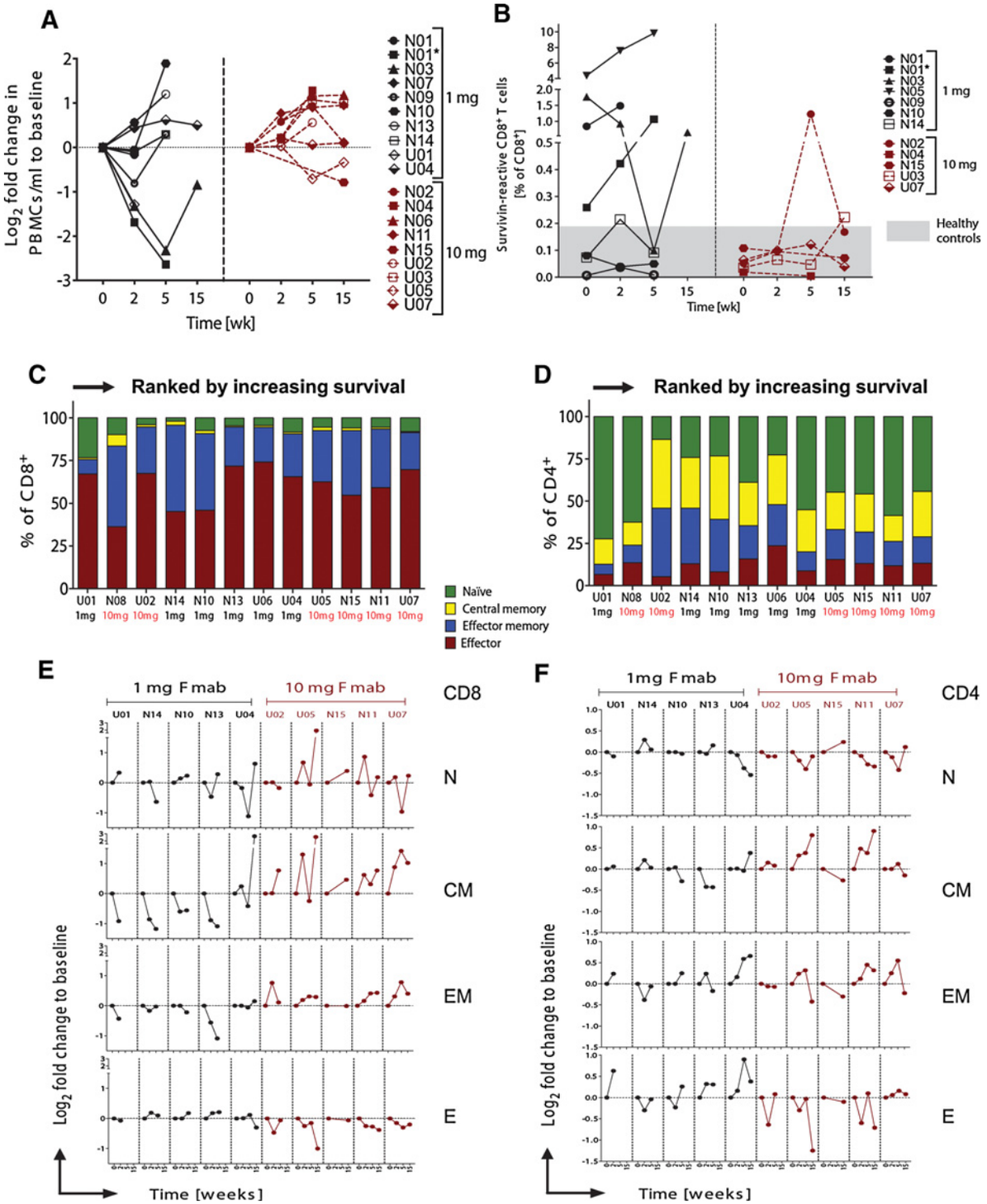

Figure 3.

Effect of TGFβ blockade on PBMC levels, survivin-reactive $CD8^+$ T cells, and memory T cells. **A,** Individual log2 fold changes in PBMC levels relative to baseline in patients receiving 1 or 10mg/kg fresolimumab. **B,** Tetramer binding data are shown as % survivin-positive $CD8^+$ T cells over the course of a 15 week treatment. The presumed threshold of median + IQR of $n = 11$ healthy control levels is indicated in gray. (N = NYU patient; U = UCLA patient; black = 1 mg and red = 10 mg fresolimumab, green = 11 healthy donors. N01 and N01* indicates repeated draws at week 0 and week 2 due to significant treatment delay). **C–F,** T-cell differentiation was assessed within each $CD4^+$ or $CD8^+$ T-cell pool giving naïve (N, $CCR7^+CD45RA^+$), central memory (CM, $CCR7^+CD45RA^-$), effector memory (EM, $CCR7^-CD45RA^-$), and effector cells (E, $CCR7^-CD45RA^+$) T cells. Data are shown as individual baseline values ranked according to survival in **C**) the $CD8^+$ compartment or **D**) the $CD4^+$ compartment or as log2 fold change to baseline in **E** and **F**, respectively.

memory pool began to diminish relative to a rising effector pool (Fig. 3E) (1 mg vs. 10 mg, week 0–2: CM $W = 16.0/P = 0.027$; EM $W = 15.0/P = 0.014$ and Effector $W = 10.0/P = 0.014$; week 0–5: CM $W = 10.0/P = 0.021$; EM $W = 10.0/P = 0.021$ and Effector $W = 10.0/P = 0.021$). This was echoed by similar tendencies in the CD4 compartment, although here there was less consistency (Fig. 3F).

Regulatory networks

Powerful regulatory networks exist to moderate immune responses and can mirror immune activation, both in timing and magnitude. Enumeration of suppressor subsets is not restricted by HLA and therefore more samples (19 in total and 20 response patterns because of N01's treatment delay) were available for analysis, increasing statistical rigor. For most patients baseline levels of T regulatory cells (Tregs) were below those of 11 healthy volunteers (med/IQR 2.55 ± 1.57% vs. 4.6 ± 1.5%; $P < 0.001$; Fig. 4A). Many showed an early rise 2 weeks after treatment initiation (2.84 ± 0.378 vs. 3.93 ± 0.454; $P = 0.005$; Fig. 4B), which was more common in the 10mg/kg-arm (6/7; 86%) compared to 6 of 11 (55%) in the 1 mg/kg arm ($W = 73.0/P = 0.004$; Fig. 4B). This is also reflected in the extent of co-tracking for Tregs alongside survivin-reactive T cells, which appeared more common in the higher antibody dose group (Fig. 4C).

Suppressor cells of the myeloid compartment followed a pattern diametrically opposed to Tregs. Most patients in the 10 mg/kg group (5/7; 71%) responded with declining monocytic myeloid-derived suppressor cells (mMDSC) within 2 weeks whereas only 36% (4 of 11) of patients in the 1 mg/kg group (Tregs/mMDSC ratio, $W = 80.0/P = 0.026$ week 0–2 and $W = 48.0/P = 0.036$ week 0—5; Fig. 4D). In other words, 64% to 75% of all patients had Treg and mMDSC trends that contrasted one another, at least initially (Supplementary Fig. S5A–S5C). The early treatment-related decline in MDSCs was also true for the granulocytic subset (gMDSCs) regardless of the drug dose given (13/18, 72%; Fig. 4E). The overall levels of gMDSCs varied widely at baseline around a med/IQR of 0.54 ± 1.23% for all patients (Supplementary Fig. S5B), which was somewhat above what was seen in healthy volunteers (0.36 ± 0.21%; $P = 0.53$).

L-Tryptophan catabolism

Activity of indoleamine 2,3-dioxygenase (IDO) or tryptophan 2,3-dioxygenase (TDO) results in a deficit in L-tryptophan and an excess in kynurenine which is commonly observed in cancer patients, presumably decreasing their T-cell viability and function. The balance of plasma tryptophan and kynurenine can be a biomarker for disease activity and response to therapy but also a gage of general inflammatory status. Carefully collected plasma in highly-inert CTAD-tubes allowed us to detect L-tryptophan and kynurenine at the expected micro-molar range of 20 to 98 and 2 to 9 μmol/L, respectively (Supplementary Fig. S6A). Samples were analyzed in two separate batches according to the study location and varied significantly. Patients treated at UCLA tended to have higher L-tryptophan and lower kynurenine than NYU's patients, resulting in lower kynurenine-to-L-tryptophan ratios at baseline (Supplementary Fig. S6A, bottom). Reasons for this difference are not clear. Regardless of location and/or treatment arm, the majority of patients responded with an early and progressive fall in plasma levels of L-tryptophan (Supplementary Fig. S6B, top; mean 61.3 ± 3.13 vs. 51.91 ± 4.09 vs. 43.48 ± 4.4; $P = 0.003$). Many, but not all, patients had a concomitant decline in kynurenine and those that did not were all treated at NYU (Supplementary Fig. S6B middle, mean = 3.53 ± 0.52 vs. 2.91 ± 0.44 vs. 2.89 ± 0.45; $P = 0.025$). Ultimately, it is the balance between these metabolites that determines the extent of immune suppression and the proportion of patients showing an encouraging shift of this balance in favor of L-tryptophan and presumably lessened suppression was higher in the 10 mg group with five of seven (71%) falling K/T ratio at week 2 versus six of 11 (55%) in the 1 mg group, although outside statistical significance (Supplementary Fig. S6B, bottom).

Summary of response patterns

The aim to find patterns of responses within complex immune monitoring data can be rewarding and challenging in equal measures. In an attempt to dissect the impact of treatment on each endpoint we used polar graphs to provide a summary of the most striking and consistent response patterns (Fig. 5). This gives us a bird's eye view of the median relative change for each endpoint between 0 and 2 weeks (Fig. 5A) and 0 and 5 weeks (Fig. 5B). Clearly, trends in Tregs ($W=73.0/P = 0.004$), in the Tregs/mMDSC ratio ($W = 80.0/P = 0.026$), in central memory CD8s ($W = 16.0/P = 0.027$), effector CD8s ($W = 10.0/P = 0.014$), in the ratio of kynurenine to tryptophan (n.s.) and in PBMC counts ($W = 70.0/P = 0.051$) yielded some of the biggest differences between the treatment arms.

Discussion

Many tumors make large amounts of TGFβ that is highly immunosuppressive and effectively blocking of TGFβ is as a result challenging. Targeting TGFβ function is even more difficult due to the diverse roles this cytokine plays. The rationale to examine TGFβ blockade by antibody in the context of metastatic breast cancer irradiation came from preclinical studies that suggested increased potential of *in situ* tumor vaccination and abscopal effects at distant tumor (26).

Clinical response was limited to stable disease in three patients. The general lack of abscopal responses (the main endpoint of the trial) implies that, at this advanced stage of breast cancer other barriers prevent immune-mediated tumor rejection. However, overall median survival was longer for patients who received the higher dose of fresolimumab, compared to those randomized to 1 mg/kg, without increased adverse events at the higher dose. Interestingly, among these women keratoacanthomas occurred, demonstrating an association of the higher dose with subversion of the TGFβ physiological role, as demonstrated before (24, 39, 40). Genetic variants in the TGFBR1 gene have been associated with multiple self-healing squamous epithelioma (MSSE), an autosomal dominant skin disease that predisposes to squamous carcinomas incidence, that then spontaneously resolve (41). The keratoacanthomas in the patients of this trial also resolved once fresolimumab was discontinued.

The difference in median overall survival associated with the higher dose needs to be interpreted with extreme caution, because the number of patients in this study was small and there was no control arm with best of standard care. In spite of these caveats, several interesting findings emerged from monitoring the immune status in these patients.

The detailed immunological analyses shown here indicated that patients in the 10 mg/kg arm responded to TGFβ blockade

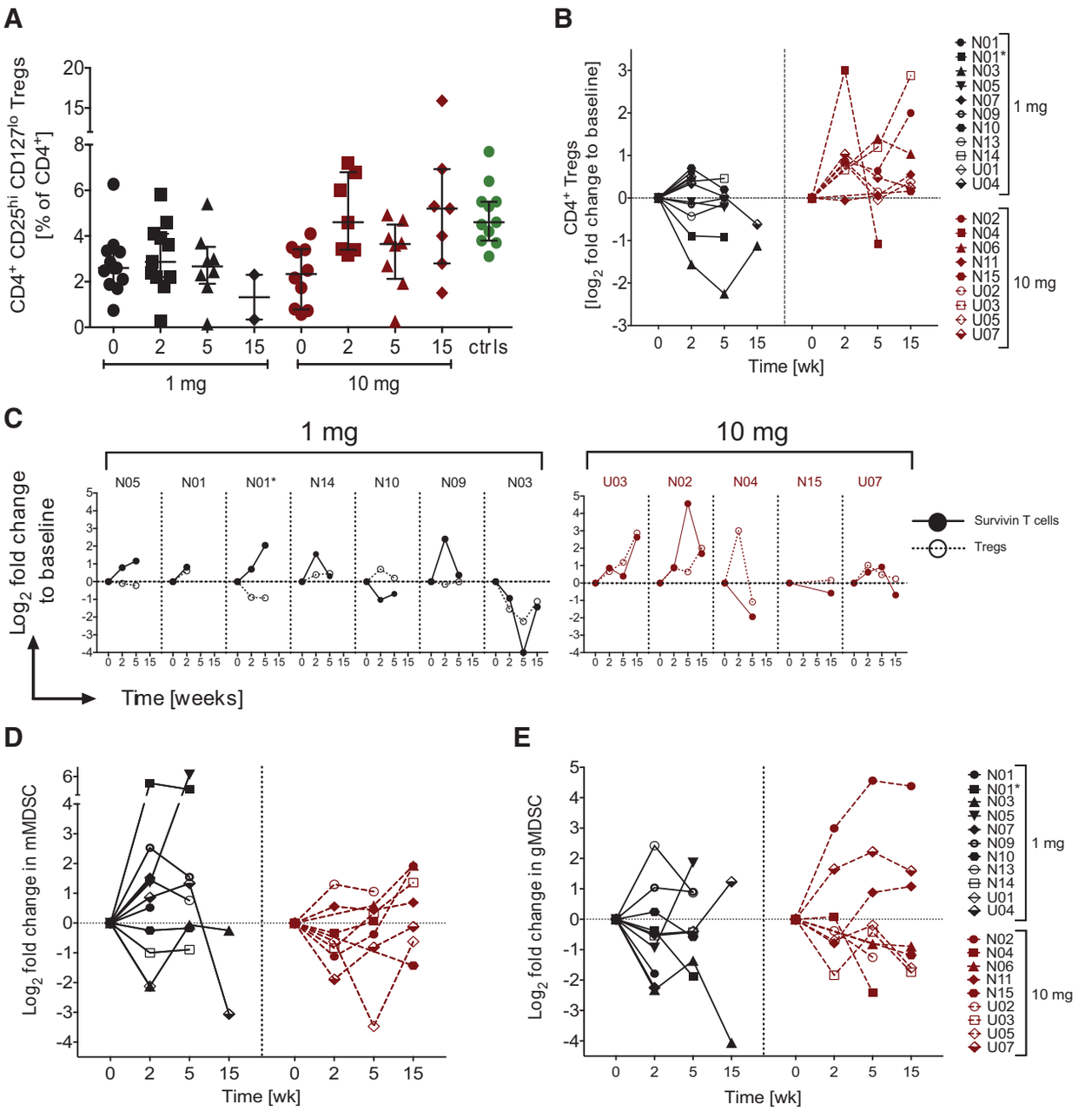

Figure 4.

High-dose TGFβ blockade combined with radiation reduces regulatory networks within the myeloid compartment while boosting Tregs. **A,** Data are % of CD4 cells that highly express CD25 while being low or negative for CD127 as individual points or (**B**) as log2 fold change to individual's baseline values. **C,** Individual log2 fold changes in $CD4^+$ Tregs side-by-side survivin-reactive $CD8^+$ T cells changes in patients ranked according to increasing survival within each treatment arm. **D,** Myeloid cells with the monocytic ($CD14^+DR^-CD16^-$) or (**E**) the granulocytic ($CD15^+DR^-CD14^-CD11b+$) myeloid-derived suppressor cell profile are shown as relative change over time to individual's baseline values. (N = treated at NYU; U = treated at UCLA; black = 1 mg and red = 10 mg fresolimumab, green = 11 healthy volunteers).

with an early, almost uniform rise in circulating Tregs. This may seem counterintuitive because TGFβ is known to support the survival and maintenance of Tregs, but it does so while also inhibiting their proliferation (42). The Treg levels appeared to be oscillating in our patients, which may have been due to the concomitant loss in survival cues necessary to maintain their levels or due to intermittent recovery in TGFβ. Whether such Treg spikes relate to inadequate antitumor immunity and poor outcomes, as one would expect in breast cancer, remains to be determined (43, 44). Our results also suggest that TGFβ blockade

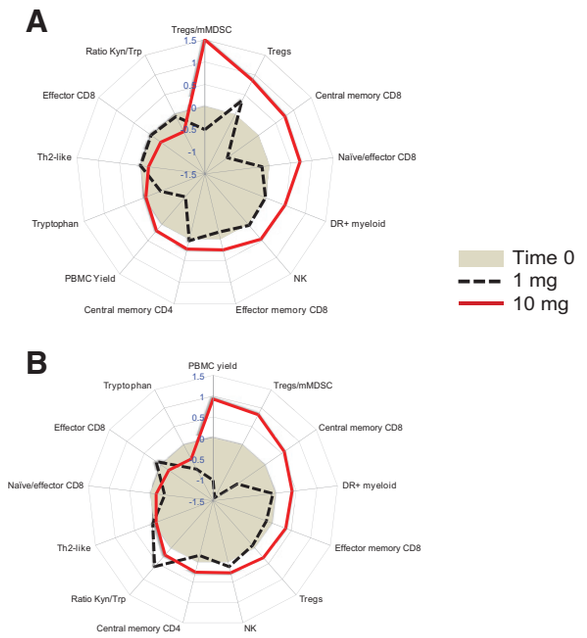

Figure 5.

Systemic TGFβ blockade and local hypofractionated radiation evoke immunologic response patterns that correlate with antibody dose. Polar graphs illustrating the median log2 fold changes during (**A**) week 0–2 and (**B**) week 0–5 for those endpoints that were different between treatment arms (gray circle = 0 (baseline), >0 increase; <0 decrease, solid red line =10 mg fresolimumab; dotted black line = 1 mg fresolimumab).

may have interrupted the IDO-Treg-MDSC axis that tends to move in unison when driving systemic immune suppression (45). Even though circulating levels of tryptophan fell and Tregs rose in most patients, suggestive of heightened IDO/TDO activity, this appeared to be uncoupled from the shrinking MDSC pool, especially in the 10 mg/kg arm. That there is a cross-talk between Tregs and MDSCs has been suggested by others (46) but how much this depends on TGFβ is unclear. Our data suggest it may provide that link. TGFβ undoubtedly drives an extensive regulatory network that strictly controls central T-cell development and tolerance as well as T-cell homeostasis and differentiation in the periphery (42).

Perhaps one of the most intriguing findings of this study pertains to T-cell homeostasis and differentiation and the fact that high-dose anti-TGFβ antibody boosted the CD8 memory pool, especially the central memory type, to the detriment of T effector cells. Similar findings have been reported in preclinical tumor models where genetic targeting of TGFβ signaling promoted memory T-cell development locally as well as systemically (47). The notion that TGFβ puts a limit on central memory development in human blood is not new and clearly speaks to the crucial role this pleiotropic cytokine plays in T-cell homeostasis (48), but it is interesting that this can be seen in humans undergoing TGFβ blockade. T-cell inflammation of the memory type also correlates with better prognosis in colorectal cancer presumably through stronger recall responses (49).′ In fact, it seems that CD8 memory T cells infiltration into the tumor site might be part of what is needed to turn an immunotherapy patient into a responder (50).

It is tempting to ascribe the difference in median overall survival between the 10 mg/kg arm and the 1 mg/kg to the immune effects in supporting a memory CD8 T-cell response and decreased MDSCs. In reality the limited patient pool and their relatively short survival times overall make this debatable. In spite of the altered immunity, it is also clear, that blocking TGFβ alone is unlikely to be sufficient in controlling tumor growth even when combined with radiation and that this approach is likely to be but one element within a cohesive, multimodal therapeutic strategy.

Disclosure of Potential Conflicts of Interest

S. Hurvitz reports receiving commercial research grants from Amgen, Bayer, Biomarin, BI Pharma, Cascadian, Dignatana, Genentech, GlaxoSmithKline, Lilly, Medivation, Merrimack, Novartis, OBI Pharma, Pfizer, PUMA, Roche, and Seattle Genetics. B. Comin-Anduix reports receiving commercial research grants from Kite Pharma, is a consultant/advisory board member for PACT Pharma, and is an external consultant for the Institutional Biosafety Committee (IBC) Schulman. S. Demaria is a consultant/advisory board member for AbbVie, Eisai, and Lytix Biopharma. No potential conflicts of interest were disclosed by the other authors.

Authors' Contributions

Conception and design: S.C. Formenti, S. Adams, J.D. Goldberg, S. Demaria, W.H. McBride

Development of methodology: S.C. Formenti, J.D. Goldberg, K.F. Faull, B. Comin-Anduix, D. Schaue

Acquisition of data (provided animals, acquired and managed patients, provided facilities, etc.): S.C. Formenti, P. Lee, S. Adams, M.W. Xie, J.A. Ratikan, C. Felix, L. Hwang, K.F. Faull, S. Hurvitz, S. Demaria, D. Schaue

Analysis and interpretation of data (e.g., statistical analysis, biostatistics, computational analysis): S.C. Formenti, P. Lee, S. Adams, J.D. Goldberg, X. Li, M.W. Xie, J.A. Ratikan, L. Hwang, J.W. Sayre, J.A. Glaspy, S. Demaria, D. Schaue

Writing, review, and/or revision of the manuscript: S.C. Formenti, P. Lee, S. Adams, J.D. Goldberg, X. Li, K.F. Faull, S. Hurvitz, J.A. Glaspy, S. Demaria, D. Schaue, W.H. McBride

Administrative, technical, or material support (i.e., reporting or organizing data, constructing databases): S.C. Formenti, P. Lee, J.D. Goldberg, J.A. Ratikan, C. Felix

Study supervision: S.C. Formenti, P. Lee, C. Felix, W.H. McBride

Acknowledgments

This study was supported by a multiteam award from the DOD CDMRP Breast cancer research program to S.C. Formenti (W81XWH-11-1-0530) and W. H. McBride (W81XWH-11-1-0531). Additional funding came from the NIH to D. Schaue (1R01CA191234-01). Additional funding was provided by the Breast Cancer Research Foundation to S.C. Formenti and S. Demaria. J.D. Goldberg and X. Li received partial support from the NYUCI CCSG 5P30CA16087 through the Biostatistics Shared Resource. The Immune Monitoring Core is partially supported by the NYU-HHC CTSI Grant, UL1 TR000038 and the NYU Cancer Institute's Cancer Center Support Grant, P30CA016087.

We would like to express our sincere thanks to all our patients. We are deeply indebted to you. Our thanks also go to the Breast Cancer Advocates involved in the design and conduction of the study: Michelle Rakoff, Jane Perlmutter, Virginia Mason, and Amy Bonoff (in memoriam). We are also extremely grateful to the NYU and UCLA clinical research teams led by Maria Fenton-Kerimian, NP and Vincent Basehart, for their outstanding care of patients and Sharanya Chandrasekhar for data managing. Further, we thank the immune monitoring core of the NYU School of Medicine for PBMC isolation from patients' blood, and the technical support of BD Biosciences, namely Dr. Ravi Hingorani during the optimization of multicolor flow cytometry was truly outstanding. Fresolimumab (GC 1008) was provided by Sanofi-Genzyme.

The costs of publication of this article were defrayed in part by the payment of page charges. This article must therefore be hereby marked *advertisement* in accordance with 18 U.S.C. Section 1734 solely to indicate this fact.

Received November 7, 2017; revised January 3, 2018; accepted February 19, 2018; published first February 23, 2018.

References

1. Blobe GC, Schiemann WP, Lodish HF. Role of transforming growth factor beta in human disease. N Engl J Med 2000;342:1350–8.
2. Dumont N, Arteaga CL. Transforming growth factor-beta and breast cancer: Tumor promoting effects of transforming growth factor-beta. Breast Cancer Res 2000;2:125–32.
3. Akhurst RJ.TGF-beta antagonists: why suppress a tumor suppressor? J Clin Invest 2002;109:1533–6.
4. Dumont N, Arteaga CL. Targeting the TGF beta signaling network in human neoplasia. Cancer Cell 2003;3:531–6.
5. Ivanovic V, Melman A, Davis-Joseph B, Valcic M, Geliebter J. Elevated plasma levels of TGF-beta 1 in patients with invasive prostate cancer. Nat Med 1995;1:282–4.
6. Junker U, Knoefel B, Nuske K, Rebstock K, Steiner T, Wunderlich H, et al. Transforming growth factor beta 1 is significantly elevated in plasma of patients suffering from renal cell carcinoma. Cytokine 1996;8:794–8.
7. Tsushima H, Kawata S, Tamura S, Ito N, Shirai Y, Kiso S, et al. High levels of transforming growth factor beta 1 in patients with colorectal cancer: association with disease progression. Gastroenterology 1996;110: 375–82.
8. Arteaga CL, Hurd SD, Winnier AR, Johnson MD, Fendly BM, Forbes JT. Anti-transforming growth factor (TGF)-beta antibodies inhibit breast cancer cell tumorigenicity and increase mouse spleen natural killer cell activity. Implications for a possible role of tumor cell/host TGF-beta interactions in human breast cancer progression. J Clin Invest 1993;92:2569–76.
9. Kobie JJ, Wu RS, Kurt RA, Lou S, Adelman MK, Whitesell LJ, et al. Transforming growth factor beta inhibits the antigen-presenting functions and antitumor activity of dendritic cell vaccines. Cancer Res 2003;63: 1860–64.
10. Lee JC, Lee KM, Kim DW, Heo DS. Elevated TGF-beta1 secretion and down-modulation of NKG2D underlies impaired NK cytotoxicity in cancer patients. J Immunol 2004;172:7335–40.
11. Ludviksson BR, Seegers D, Resnick AS, Strober W. The effect of TGF-beta1 on immune responses of naive versus memory CD4+ Th1/Th2 T cells. Eur J Immunol 2000;30:2101–11.
12. Woo EY, Chu CS, Goletz TJ, Schlienger K, Yeh H, Coukos G, et al. Regulatory CD4(+)CD25(+) T cells in tumors from patients with early-stage non-small cell lung cancer and late-stage ovarian cancer. Cancer Res 2001;61:4766–72.
13. Tada T, Ohzeki S, Utsumi K, Takiuchi H, Muramatsu M, Li XF, et al. Transforming growth factor-beta-induced inhibition of T cell function. Susceptibility difference in T cells of various phenotypes and functions and its relevance to immunosuppression in the tumor-bearing state. J Immunol 1991;146:1077–82.
14. Demaria S, Bhardwaj N, McBride WH, Formenti SC. Combining radiotherapy and immunotherapy: a revived partnership. Int J Radiat Oncol Biol Phys 2005;63:655–66.
15. McBride WH, Chiang C-S, Olson JL, Wang C-C, Hong J-H, Pajonk F, et al. A sense of danger from radiation. Radiat Res 2004;162:1–19.
16. Liao YP, Wang CC, Butterfield LH, Economou JS, Ribas A, Meng WS, et al. Ionizing radiation affects human MART-1 melanoma antigen processing and presentation by dendritic cells. J Immunol 2004;173:2462–9.
17. Barcellos-Hoff MH. Radiation-induced transforming growth factor beta and subsequent extracellular matrix reorganization in murine mammary gland. Cancer Res 1993;53:3880–6.
18. Hauer-Jensen M, Richter KK, Wang J, Abe E, Sung CC, Hardin JW. Changes in transforming growth factor beta1 gene expression and immunoreactivity levels during development of chronic radiation enteropathy. Radiat Res 1998;150:673–80.
19. Becker KA, Lu S, Dickinson ES, Dunphy KA, Mathews L, Schneider SS, et al. Estrogen and progesterone regulate radiation-induced p53 activity in mammary epithelium through TGF-beta-dependent pathways. Oncogene 2005;24:6345–53.
20. Milliat F, Francois A, Isoir M, Deutsch E, Tamarat R, Tarlet G, et al. Influence of endothelial cells on vascular smooth muscle cells phenotype after irradiation: implication in radiation-induced vascular damages. Am J Pathol 2006;169:1484–95.
21. Tabatabai G, Frank B, Mohle R, Weller M, Wick W. Irradiation and hypoxia promote homing of haematopoietic progenitor cells towards gliomas by TGF-beta-dependent HIF-1alpha-mediated induction of CXCL12. Brain 2006;129:2426–35.
22. Jobling MF, Mott JD, Finnegan MT, Jurukovski V, Erickson AC, Walian PJ, et al. Isoform-specific activation of latent transforming growth factor beta (LTGF-beta) by reactive oxygen species. Radiat Res 2006;166:839–48.
23. Barcellos-Hoff MH, Cucinotta FA. New tricks for an old fox: impact of TGFbeta on the DNA damage response and genomic stability. Sci Signal 2014;7:re5.
24. Morris JC, Tan AR, Olencki TE, Shapiro GI, Dezube BJ, Reiss M, et al. Phase I study of GC1008 (fresolimumab): a human anti-transforming growth factor-beta (TGFbeta) monoclonal antibody in patients with advanced malignant melanoma or renal cell carcinoma. PLoS One 2014;9:e90353.
25. Bouquet F, Pal A, Pilones KA, Demaria S, Hann B, Akhurst RJ, et al. TGFβ1 inhibition increases the radiosensitivity of breast cancer cells in vitro and promotes tumor control by radiation in vivo. Clin Cancer Res 2011; 17:6754–65.
26. Vanpouille-Box C, Diamond JM, Pilones KA, Zavadil J, Babb JS, Formenti SC, et al. TGFbeta is a master regulator of radiation therapy-induced antitumor immunity. Cancer Res 2015;75:2232–42.
27. Wolchok JD, Hoos A, O'Day S, Weber JS, Hamid O, Lebbé C, et al. Guidelines for the evaluation of immune therapy activity in solid tumors: immune-related response criteria. Clin Cancer Res 2009;15:7412–20.
28. Maecker HT, McCoy JP, Nussenblatt R. Standardizing immunophenotyping for the human immunology project. Nat Rev Immunol 2012;12:191–200.
29. Andersen MH, Pedersen LO, Capeller B, Brocker EB, Becker JC, thor Straten P. Spontaneous cytotoxic T-cell responses against survivin-derived MHC class I-restricted T-cell epitopes in situ as well as ex vivo in cancer patients. Cancer Res 2001;61:5964–8.
30. Schaue D, Comin-Anduix B, Ribas A, Zhang L, Goodglick L, Sayre JW, et al. T-cell responses to survivin in cancer patients undergoing radiation therapy. Clin Cancer Res 2008;14:4883–90.
31. Yamamoto S, Wu Z, Russnes HG, Takagi S, Peluffo G, Vaske C, et al. JARID1B is a luminal lineage-driving oncogene in breast cancer. Cancer Cell 2014;25:762–77.
32. Coleman JA, Correa I, Cooper L, Bohnenkamp HR, Poulsom R, Burchell JM, et al. T cells reactive with HLA-A*0201 peptides from the histone demethylase JARID1B are found in the circulation of breast cancer patients. Int J Cancer 2011;128:2114–24.
33. Kokowski K, Harnack U, Dorn DC, Pecher G. Quantification of the CD8(+) T cell response against a mucin epitope in patients with breast cancer. Arch Immunol Ther Exp 2008;56:141–5.
34. Mittendorf EA, Gurney JM, Storrer CE, Shriver CD, Ponniah S, Peoples GE. Vaccination with a HER2/neu peptide induces intra- and inter-antigenic epitope spreading in patients with early stage breast cancer. Surgery 2006;139:407–18.
35. Guckel B, Rentzsch C, Nastke MD, Marme A, Gruber I, Stevanovic S, et al. Pre-existing T-cell immunity against mucin-1 in breast cancer patients and healthy volunteers. J Cancer Res Clin Oncol 2006;132:265–74.
36. Domschke C, Schuetz F, Ge Y, Seibel T, Falk C, Brors B, et al. Intratumoral cytokines and tumor cell biology determine spontaneous breast cancer-specific immune responses and their correlation to prognosis. Cancer Res 2009;69:8420–8.
37. Comin-Anduix B, Gualberto A, Glaspy JA, Seja E, Ontiveros M, Reardon DL, et al. Definition of an immunologic response using the major histocompatibility complex tetramer and enzyme-linked immunospot assays. Clin Cancer Res 2006;12:107–16.
38. Midttun O, Hustad S, Ueland PM. Quantitative profiling of biomarkers related to B-vitamin status, tryptophan metabolism and inflammation in human plasma by liquid chromatography/tandem mass spectrometry. Rapid Commun Mass Spectrom 2009;23:1371–9.
39. Lacouture ME, Morris JC, Lawrence DP, Tan AR, Olencki TE, Shapiro GI, et al. Cutaneous keratoacanthomas/squamous cell carcinomas associated with neutralization of transforming growth factor beta by the monoclonal antibody fresolimumab (GC1008). Cancer Immunol Immunother 2015;64:437–46.
40. Lonning S, Mannick J, McPherson JM. Antibody targeting of TGF-beta in cancer patients. Curr Pharm Biotechnol 2011;12:2176–89.
41. Goudie DR, D'Alessandro M, Merriman B, Lee H, Szeverenyi I, Avery S, et al. Multiple self-healing squamous epithelioma is caused by a disease-specific spectrum of mutations in TGFBR1. Nat Genet 2011;43:365–9.
42. Li MO, Flavell RA. TGF-beta: a master of all T cell trades. Cell 2008;134:392–404.

43. Verma C, Eremin JM, Robins A, Bennett AJ, Cowley GP, El-Sheemy MA, et al. Abnormal T regulatory cells (Tregs: FOXP3+, CTLA-4+), myeloid-derived suppressor cells (MDSCs: monocytic, granulocytic) and polarised T helper cell profiles (Th1, Th2, Th17) in women with large and locally advanced breast cancers undergoing neoadjuvant chemotherapy (NAC) and surgery: failure of abolition of abnormal treg profile with treatment and correlation of treg levels with pathological response to NAC. J Transl Med 2013;11:16.
44. Bailur JK, Gueckel B, Derhovanessian E, Pawelec G. Presence of circulating Her2-reactive CD8 + T-cells is associated with lower frequencies of myeloid-derived suppressor cells and regulatory T cells, and better survival in older breast cancer patients. Breast Cancer Res 2015;17:34.
45. Holmgaard RB, Zamarin D, Li Y, Gasmi B, Munn DH, Allison JP, et al. Tumor-expressed IDO recruits and activates MDSCs in a treg-dependent manner. Cell Rep 2015;13:412–24.
46. Fujimura T, Kambayashi Y, Aiba S. Crosstalk between regulatory T cells (Tregs) and myeloid derived suppressor cells (MDSCs) during melanoma growth. Oncoimmunology 2012;1:1433–4.
47. Gate D, Danielpour M, Rodriguez J Jr., Kim GB, Levy R, Bannykh S, et al. T-cell TGF-beta signaling abrogation restricts medulloblastoma progression. Proc Natl Acad Sci U S A 2014;111:E3458–66.
48. Takai S, Schlom J, Tucker J, Tsang KY, Greiner JW. Inhibition of TGF-beta1 signaling promotes central memory T cell differentiation. J Immunol 2013;191:2299–307.
49. Pages F, Berger A, Camus M, Sanchez-Cabo F, Costes A, Molidor R, et al. Effector memory T cells, early metastasis, and survival in colorectal cancer. N Engl J Med 2005;353:2654–66.
50. Ribas A, Shin DS, Zaretsky J, Frederiksen J, Cornish A, Avramis E, et al. PD-1 blockade expands intratumoral memory T cells. Cancer Immunol Res 2016;4:194–203.